Nanoparticle Architectures Hot Paper

DOI: 10.1002/anie.201406854

Planet–Satellite Nanostructures Made To Order by RAFT Star Polymers**

*Christian Rossner and Philipp Vana**

Abstract: *The investigation and application of complex nanostructures requires the hierarchical arrangement of distinct domains on a small scale. Herein, we report a method to prepare planet–satellite arrangements using RAFT polymers. Our approach is based on star polymers decorated with trithiocarbonate groups on their outer periphery that attach to gold surfaces and thus provide the polymer with the ability to connect (larger) gold nanoparticle planets with (smaller) gold nanoparticle satellites. By adjusting the molecular weight of the polymeric linker, nanostructures with tailored planet–satellite distances, as evidenced by transmission electron microscopy, are obtained. This strategy offers a straightforward way to prepare gold nanoparticle scaffolds with multiple reactive functionalities at defined distances from the central core.*

Multicomponent nanoarchitectures[1] combine several distinct building units in structured nanohybrids. Besides the general human longing for aesthetic, ordered structures, the curiosity of studying emergent physical properties of such systems is another driving force in this research direction and has led to, for example, planet–satellite nanostructures. These materials in particular were suggested as platforms for sensing,[2] scaffolds for the selective functionalization of individual nanoparticles on specific sites,[3] plasmon rulers,[4] surface-enhanced Raman scattering probes,[5] and tumor-specific delivery agents.[6] However, an efficient and versatile synthetic procedure for obtaining custom-made planet–satellite particles is the prerequisite for investigating and using these architectures. In this regard, planet–satellite distances were found to be tunable within a few nanometers by increasing the length of the linking alkyl chains.[7] To achieve control over particle distances at larger length scales, the logical rational appears to be the use of well-defined polymers as cross-linking agents. DNA is a versatile biopolymer to encode nanoparticle superstructures[8] and as such, it was consequently also applied to direct the formation of planet–satellite assemblies.[9] However, using well-defined synthetic polymers instead of DNA is an efficient alternative which would avoid the laborious design and synthesis of a library of DNA linkers and would provide higher flexibility with regard to the chemical properties of the nanostructure.

RAFT polymerization[10] (reversible addition—fragmentation chain transfer) can be used to produce polymers with narrow molecular weight distributions around predetermined average values and at the same time provides a handle to control polymer topology and end-group functionality. RAFT polymers can be used directly to form nanocomposites with gold nanoparticles, as the RAFT polymers' thiocarbonylthio group was shown to act as an anchor for chemisorption on gold surfaces;[11] our lab has recently demonstrated the ability of such polymers to attach to gold nanoparticles made by citrate reduction[12] and two-phase Brust–Schiffrin (BS) synthesis.[13] Decorating gold nanoparticles with a polymer layer that allows further particles to be attached to the central core is of huge current interest in the field and hyperbranched RAFT polymers have been shown to be suitable for this task, as they provide multiple binding sites for gold statistically distributed among the thus produced macromolecules.[14] Better defined macromolecules can be obtained by employing RAFT agents with star topology.[15] When the arms of the star are joined together through their reinitiating R groups, macromolecules with the sulfur-containing RAFT groups exposed on the outer sphere of the star—and therefore accessible for functional units to be attached—will result (Scheme 1).

Based on these considerations, we fabricated star polymers of *N*-isoprylacrylamide (N^{i}PAAM) derived from RAFT agent **2** (Figure 1). PN^{i}PAAM exhibits a temperature- and pressure-dependent coil-to-globule transition[16] which was recently shown to enable the construction of "smart" gold nanoparticles.[17] More importantly for this work, it is also a polymer soluble in solvents of different nature. The synthesis of compound **2** was practically identical to a previously reported method[18] and we verified the structure of **2** by NMR spectroscopy (Figures S1 and S2). RAFT agent **1**[13] was used to prepare PN^{i}PAAM with linear topology. After isolation of the polymeric material, all samples were analyzed by size-exclusion chromatography (SEC) (Figure S3). The SE chromatograms display—if at all—only a small shoulder at higher molecular weights, suggesting that star–star coupling occurs to only a minor extent under the polymerization conditions applied. Due to the confinement of their branches to a central core, star polymers show a systematically smaller hydrodynamic radius than linear polymers of the same molecular weight, and the ratio of these two radii was derived theoretically to depend only on the number of branches.[19] In

[*] C. Rossner, Prof. Dr. P. Vana
Institut für Physikalische Chemie, Universität Göttingen
Tammannstrasse 6, 37077 Göttingen (Germany)
E-mail: pvana@uni-goettingen.de
Homepage: http://www.mmc.chemie.uni-goettingen.de

[**] We thank Dr. Florian Ehlers for designing the table of contents artwork and Dr. Jens Grosche, Effigos AG Leipzig (Germany) for the design of the synthetic scheme. Generous financial support by the Fonds der Chemischen Industrie (PhD fellowship to C.R.) is gratefully acknowledged. P.V. thanks the DFG for a Heisenberg Professorship (DFG). RAFT = reversible addition—fragmentation chain transfer.

Supporting information for this article is available on the WWW under http://dx.doi.org/10.1002/anie.201406854.

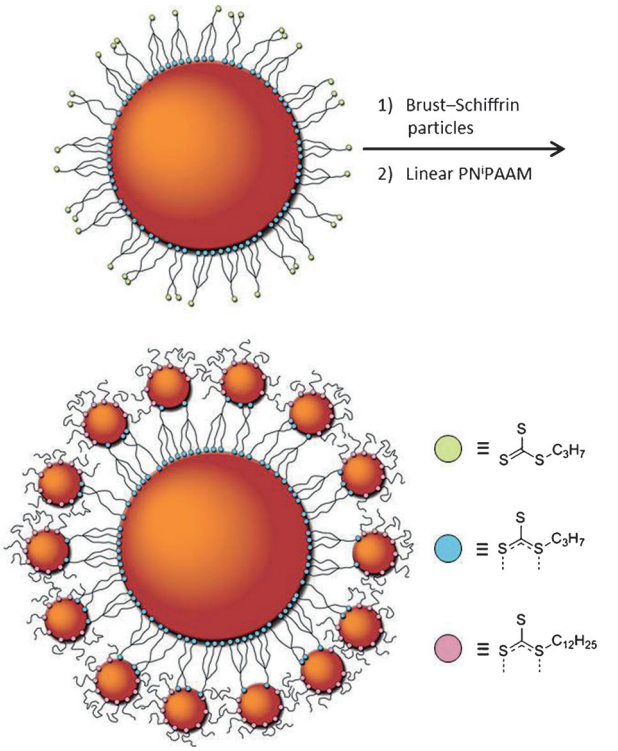

Scheme 1. Synthetic scheme for the preparation of planet–satellite particles from nanohybrid particles by citrate reduction with star polymers of N^{i}PAAM (top, surface-bound and free RAFT groups are indicated by blue and green circles, respectively). The ω-end groups of linear PN^{i}PAAM are represented by pink circles.

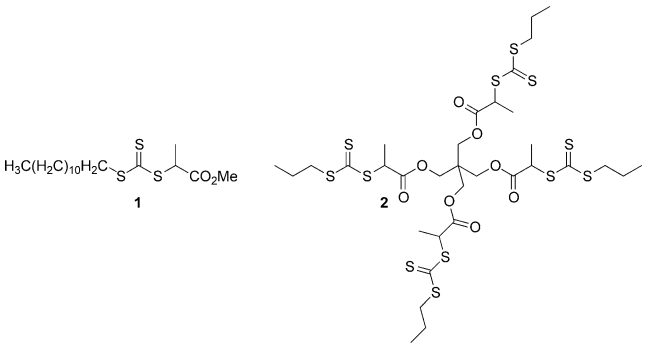

Figure 1. RAFT agents used in this study for the preparation of linear (**1**) and star-shaped polymers (**2**).

earlier studies, we were able to determine a correction factor for star polymers (including polymers with four branches) measured on an SEC setup calibrated using linear standards and the results from SEC obtained for this study were thus corrected by multiplication with this factor (1.3).[20] The results of SEC analysis are given in Table 1.

The as-prepared star polymers (a–p) were subsequently used to cover gold nanocrystals from citrate reduction (13.6 nm; see Figure S5 for an exemplary TE micrograph and Figure S7 for a diameter histogram). The obtained nanohybrids α–π were centrifuged and redispersed in methanol and subsequently in dichloromethane. This procedure

Table 1: Polymerization conditions for the preparation of the different polymer samples and results from SEC analysis.[a]

Polymer	Equiv[b] of DMF	Equiv[b] of N^{i}PAAM	Equiv[b] of AIBN	t [min]	M_n (SEC)[c,d]	$Đ$ (SEC)[c]
Star-a	300	100	0.1	360	12000	1.20
Star-b	1600	400	0.4	90	22000	1.10
Star-c	1600	400	0.4	120	27000	1.11
Star-d	1600	400	0.4	180	34000	1.11
Star-e	1600	400	0.4	240	40000	1.08
Star-t	6000	1000	0.75	90	42000	1.08
Star-l	6000	1000	0.75	105	46000	1.09
Star-m	6000	1000	0.75	120	52000	1.13
Star-p	6000	1000	0.75	180	62000	1.15
Linear	2400	800	0.5	120	49000	1.18

[a] Star polymer samples a–p were derived from **2**, whereas **1** was applied in the preparation of the linear PN^{i}PAAM sample. All polymerizations were conducted at 60 °C. [b] With respect to the RAFT agent. [c] As monitored by refractive index detection. [d] The values for star polymer samples were corrected by an experimental form factor.[20]

allowed purification of the nanohybrids and also enabled solvent exchange. The nanocomposites were analyzed by TEM (Figure 2, Table S2) and DLS (Figure S8). The micrographs in Figure 2 display hexagonal patterns of self-assembled nanoparticles. Although the polymer layer cannot be visualized directly, it keeps the cores at certain distances, which grow with the increasing molecular weight of the star polymers employed in the functionalization reactions.[12] If no interdigitation of macromolecules of the individual shells occurs, then the interparticle distances should be twice as large as the polymer layer covering the gold nanoparticle. The DLS data confirm the qualitative trend found by TEM. Furthermore, DLS data reveal unimodal particle size distributions, suggesting that exclusively individual particles are present in solution, with no indication for cross-linked particle networks. We analyzed several TEM images of the different nanocomposite samples and measured edge-to-edge distances in undistorted hexagons.[12] The results reveal interparticle distances strictly increasing with the molecular weight of the star polymer (Figure 5, gray circles), strongly suggesting that the thickness of the polymer layer can be adjusted by the

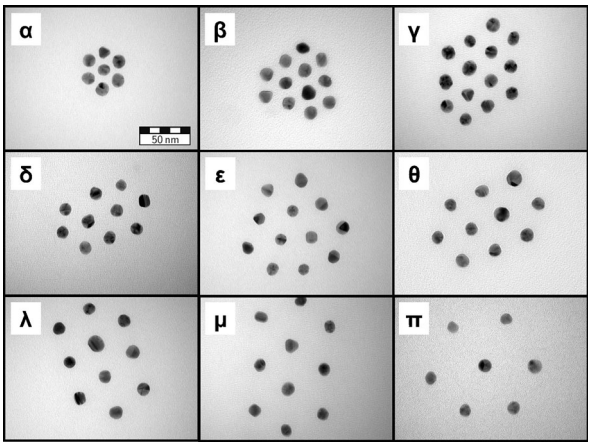

Figure 2. Hexagonally assembled layers of hybrid nanoparticles.

preceding RAFT process. The curvature of this increase gives additional information about the binding of star polymers: The data in Figure 5 show interparticle distances increasing exponentially with the molecular weight of the star polymers. This can only be explained if one assumes that the surface area covered by one macromolecule is minimized, in order to enable many attractive trithiocarbonate (TTC)–gold interactions. This would force the star polymers to adopt conformations in which their TTC termini, whether surface-bound or on the exterior of the polymer layer, are in close proximity. This effect will alter the overall shape of the star polymer, leading to elongated structures with increasing arm lengths. It is of special interest to investigate whether the star polymers bind to the citrate particles with all end groups. In particular, if some of the arms of the immobilized star polymer do not bind to the gold nanoparticle, then the TTC groups in these dangling arms should still be available for functionalization reactions.

To prove that TTC moieties are exposed at distinct distances from the gold core and furthermore accessible for functionalization reactions, tetraoctylammonium bromide (TOAB)-capped gold nanoparticles (3.8 nm) made by the two-phase BS method were added to the nanohybrids α–π in large excess. (See Figure S6 for an exemplary TE micrograph and Figure S7 for the diameter histograms of the two types of particles employed, which do not overlap). TOAB is known to be easily replaced by competitive ligands,[13,21] which implies only weak binding between TOAB and gold which may result in poor colloidal stability. Hence, in order to shield the outer hemispheres of the satellite particles which are remote from the central planet particle, linear RAFT polymer was added 10 min after addition of the BS particles.[22] After an additional 5 min the mixtures were centrifuged for 8 h at 8600 g. The supernatant almost exclusively contained individual BS particles (see Figure S9 for an exemplary TEM image), proving the excellent separation of excess satellite particles by centrifugation. The segregated material could be (although not completely) redispersed in dichloromethane by shaking. In earlier attempts, where no shielding linear polymer was employed, the redispersion failed, showing that the shielding with linear chains is crucial to obtain planet–satellite nanostructures (A–Π) with sufficient colloidal stability. Centrifugation–redispersion was repeated once in order to fully remove any unbound satellite particles. Figure 3 displays exemplary TEM images of individual planet–satellite particles. These particles also tended to arrange in two-dimensional assemblies on the TEM substrate after solvent evaporation (as can be exemplarily seen for nanostructure M in Figure 4 and for the other structures in Figure S10), although these assemblies were not as regular as those found for nanocomposites without satellite particles. The formation of planet–satellite structures proves that a significant proportion of star polymers tethered to the central gold core provide TTC moieties exposed on their polymer shell, that is, they do bind to the planet particle with less than four arms.

Planet–satellite distances were analyzed in these nanostructures and found to monotonically increase with increasing molecular weight of the star polymers employed (Figure 5, black circles, Table S3).

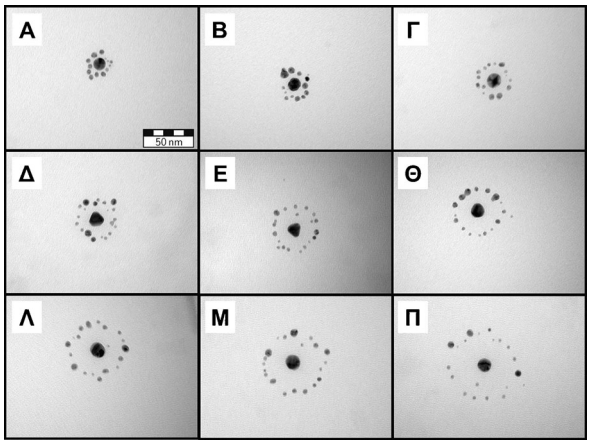

Figure 3. TE micrographs of planet–satellite nanostructures.

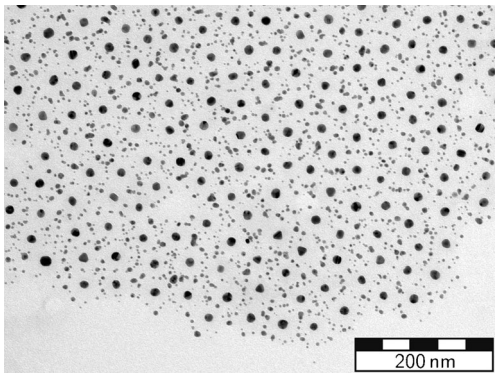

Figure 4. Exemplary micrograph of a two-dimensional assembly of planet–satellite nanostructure M.

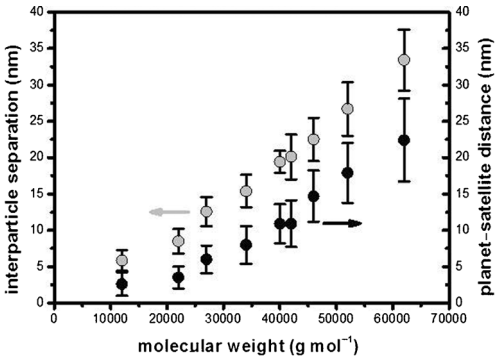

Figure 5. Edge-to-edge distances of hybrid particles α–π (gray circles) and edge-to-edge distances of planets and surrounding satellites in nanostructures A–Π (black circles).

To investigate whether the satellite particles in the nanostructures A–Π really bind on the exterior of the polymer layer, rather than being statistically incorporated inside this polymer shell, the ratio of planet–satellite distances in A–Π to the interparticle separation of nanohybrids α–π was determined. This ratio is indeed close to 0.5—as one would expect if the interparticle distances in α–π are a factor of two larger than the thickness of one polymer layer (the calculated ratios are 0.45 ± 0.39; 0.41 ± 0.26; 0.48 ± 0.23;

0.52 ± 0.25; 0.56 ± 0.19; 0.54 ± 0.25; 0.65 ± 0.25; 0.67 ± 0.25; 0.67 ± 0.26; for the star polymers a–p, respectively).

When analyzing these planet–satellite particles by DLS (Figure S8), we found unimodal size distributions for all samples A–Π, with a trend towards higher values as the molecular weight of the linking star polymer increases. Thus, the planet–satellite nanostructures can be regarded as individual units in solution, whereas the layers comprising several planet–satellite particles (Figure S10) form upon solvent evaporation on the TEM substrate.

Finally, one might suspect that the N^{i}PAAM repeating unit interacts with the gold surfaces itself, as weak N–H···Au hydrogen bonds were identified in DFT calculations employing neutral Au_3 model clusters interacting with formamide ligands.[23] Thus, we tested our synthetic strategy by employing a monomer without this structural feature (*N*,*N*-dimethylacrylamide, DMAAM; see Figure S4 for SEC traces). The formation of planet–satellite nanostructures was observed as well (Figure S12), suggesting that TTC end groups, not the monomeric repeating unit, play the dominant role in forming these arrangements.

In conclusion, we have developed a modular procedure to prepare multifunctional nanoparticle scaffolds[24] with chemical functionality exposed at set distances from the central core. This was proven by the formation of planet–satellite nanostructures when another type of particles with affinity to TTC groups was added to the system. The special value of this strategy lies in the fact that no incorporation of specialized functional groups[25]—which would add significantly to the complexity of the approach—is required, neither for attaching the polymers used to the central planets nor for connecting them to satellite particles. Rather, the TTC group, which is inherently present in this kind of polymer, is exploited for functionalization reactions in a very straightforward manner. Given the fact that a plethora of efficient TTC group transformations are available,[26] this approach offers a general route to precise nanoparticle modification with an array of possible reactions.

Received: July 3, 2014
Published online: August 19, 2014

Keywords: colloids · gold · nanostructures · RAFT · star polymers

[1] T.-D. Nguyen, T.-H. Tran, *RSC Adv.* **2014**, *4*, 916 – 942.
[2] I. Choi, H. D. Song, S. Lee, Y. I. Yang, T. Kang, J. Yi, *J. Am. Chem. Soc.* **2012**, *134*, 12083 – 12090.
[3] X. Xu, N. L. Rosi, Y. Wang, F. Huo, C. A. Mirkin, *J. Am. Chem. Soc.* **2006**, *128*, 9286 – 9287.
[4] Y.-w. Jun, S. Sheikholeslami, D. R. Hostetter, C. Tajon, C. S. Craik, A. P. Alivisatos, *Proc. Natl. Acad. Sci. USA* **2009**, *106*, 17735 – 17740.
[5] N. Gandra, A. Abbas, L. Tian, S. Singamaneni, *Nano Lett.* **2012**, *12*, 2645 – 2651.
[6] L. Y. T. Chou, K. Zagorovsky, W. C. W. Chan, *Nat. Nanotechnol.* **2014**, *9*, 148 – 155.
[7] a) J. H. Yoon, J. Lim, S. Yoon, *ACS Nano* **2012**, *6*, 7199 – 7208; b) J. H. Yoon, Y. Zhou, M. G. Blaber, G. C. Schatz, S. Yoon, *J. Phys. Chem. Lett.* **2013**, *4*, 1371 – 1378; c) J. H. Yoon, S. Yoon, *Langmuir* **2013**, *29*, 14772 – 14778.
[8] a) S. Y. Park, A. K. R. Lytton-Jean, B. Lee, S. Weigand, G. C. Schatz, C. A. Mirkin, *Nature* **2008**, *451*, 553 – 556; b) C. Zhang, R. J. Macfarlane, K. L. Young, C. H. J. Choi, L. Hao, E. Auyeung, G. Liu, X. Zhou, C. A. Mirkin, *Nat. Mater.* **2013**, *12*, 741 – 746.
[9] R. Schreiber, J. Do, E.-M. Roller, T. Zhang, V. J. Schüller, P. C. Nickels, J. Feldmann, T. Liedl, *Nat. Nanotechnol.* **2014**, *9*, 74 – 78.
[10] J. Chiefari, Y. K. Chong, F. Ercole, J. Krstina, J. Jeffery, T. P. T. Le, R. T. A. Mayadunne, G. F. Meijs, C. L. Moad, G. Moad, E. Rizzardo, S. H. Thang, *Macromolecules* **1998**, *31*, 5559 – 5562.
[11] a) A.-S. Duwez, P. Guillet, C. Colard, J.-F. Gohy, C.-A. Fustin, *Macromolecules* **2006**, *39*, 2729 – 2731; b) C.-A. Fustin, C. Colard, M. Filali, P. Guillet, A.-S. Duwez, M. A. R. Meier, U. S. Schubert, J.-F. Gohy, *Langmuir* **2006**, *22*, 6690 – 6695.
[12] B. Ebeling, P. Vana, *Macromolecules* **2013**, *46*, 4862 – 4871.
[13] C. Rossner, B. Ebeling, P. Vana, *ACS Macro Lett.* **2013**, *2*, 1073 – 1076.
[14] a) P. Dey, I. Blakey, K. J. Thurecht, P. M. Fredericks, *Langmuir* **2013**, *29*, 525 – 533; b) P. Dey, I. Blakey, K. J. Thurecht, P. M. Fredericks, *Langmuir* **2014**, *30*, 2249 – 2258; c) P. Dey, S. Zhu, K. J. Thurecht, P. M. Fredericks, I. Blakey, *J. Mater. Chem. B* **2014**, *2*, 2827 – 2837.
[15] D. Boschmann, P. Vana, *Macromolecules* **2007**, *40*, 2683 – 2693.
[16] B. Ebeling, S. Eggers, M. Hendrich, A. Nitschke, P. Vana, *Macromolecules* **2014**, *47*, 1462 – 1469.
[17] K. Zhang, X. Zhu, E. Auyeung, C. A. Mirkin, *J. Am. Chem. Soc.* **2013**, *135*, 14102 – 14105.
[18] K. O. Sebakhy, M. Gavrilov, D. Valade, Z. Jia, M. J. Monteiro, *Macromol. Rapid Commun.* **2014**, *35*, 193 – 197.
[19] M. Daoud, J. P. Cotton, *J. Phys. (Paris)* **1982**, *43*, 531 – 538.
[20] a) D. Boschmann, R. Edam, P. J. Schoenmakers, P. Vana, *Polymer* **2008**, *49*, 5199 – 5208; b) D. Boschmann, R. Edam, P. J. Schoenmakers, P. Vana, *Macromol. Symp.* **2009**, *275 – 276*, 184 – 196.
[21] J. Zhou, D. A. Beattie, R. Sedev, J. Ralston, *Langmuir* **2007**, *23*, 9170 – 9177.
[22] L. Zhang, Y. Xu, H. Yao, L. Xie, J. Yao, H. Lu, P. Yang, *Chem. Eur. J.* **2009**, *15*, 10158 – 10166.
[23] a) E. S. Kryachko, F. Remacle, *Chem. Phys. Lett.* **2005**, *404*, 142 – 149; b) H. Schmidbaur, H. G. Raubenheimer, L. Dobrzańska, *Chem. Soc. Rev.* **2014**, *43*, 345 – 380.
[24] C. Fasting, C. A. Schalley, M. Weber, O. Seitz, S. Hecht, B. Koksch, J. Dernedde, C. Graf, E.-W. Knapp, R. Haag, *Angew. Chem.* **2012**, *124*, 10622 – 10650; *Angew. Chem. Int. Ed.* **2012**, *51*, 10472 – 10498.
[25] N. Gandra, S. Singamaneni, *Chem. Commun.* **2012**, *48*, 11540 – 11542.
[26] G. Moad, E. Rizzardo, S. H. Thang, *Polym. Int.* **2011**, *60*, 9 – 25.

